Copyright WILEY-VCH Verlag GmbH & Co. KGaA, 69469 Weinheim, Germany, 2016.

Supporting Information

Efficient charge carrier injection and balance achieved by low electrochemical doping in solution-processed polymer light-emitting diodes

Hao Yan, Saurav Limbu, Xuhua Wang, James Nightingale, Iain Hamilton, Jessica Wade, Sooncheol Kwon, Kwanghee Lee* and Ji-Seon Kim**

Table 1. Summary of neat F8BT and F8BT:EDA (0.5 wt% blend) PLED performances with thicknesses from 60 nm to 1200 nm showing turn-on voltage (V_J and V_L), current density (mA/cm^2) and luminance (cd/m^2) at certain voltages, peak luminous efficiency (cd/A) and peak power efficiency (lm/W). The turn-on voltages of F8BT:EDA devices with low thicknesses (60 nm to 200 nm) are much less thickness-dependent.

Thickness (nm)	Turn-on voltage (V)				Current density (mA/cm^2) at V		Luminance (cd/m^2) at V		Peak luminous efficiency (cd/A)		Peak power efficiency (lm/W)	
	current density (J)		Luminance (L)									
	Neat	Blend	Neat	Blend	Neat	Blend	Neat	Blend	Neat	Blend	Neat	Blend
60 nm	1.7	1.7	2.0	1.9	835 (8 V)	735 (8 V)	54210	45380	7.4 (3.9 V)	6.7 (3.7 V)	7.0 (3.2 V)	6.5 (3 V)
70 nm	1.8	1.7	2.1	2.0	742 (8 V)	877 (8 V)	47740	56670	7.9 (4 V)	7.3 (3.8 V)	7.1 (3.2 V)	7.0 (2.8 V)
90 nm	1.9	1.7	2.4	2.0	527 (8 V)	744 (8 V)	20840	35510	4.8 (4.4 V)	5.2 (4.2 V)	3.7 (3.8 V)	4.6 (3 V)
100 nm	2.1	1.7	2.6	2.1	379 (8 V)	684 (8 V)	12490	26110	4.1 (4.4 V)	4.2 (4.4 V)	3.0 (3.8 V)	3.8 (3 V)
112 nm	2.2	1.8	2.9	2.2	191 (8 V)	586 (8 V)	3385	14880	2.0 (5.4 V)	2.8 (4.6 V)	1.3 (4.6 V)	2.2 (3.4 V)
200 nm	3.6	2.0	4.2	2.9	31 (8 V)	67 (8V)	1026	4195	3.3 (7 V)	6.4 (6.8 V)	1.6 (6 V)	3.4 (5.2 V)
650 nm	9.1	5.6	9.4	6.9	137 (28 V)	113 (28 V)	10910	7611	8.3 (18 V)	7.0 (17 V)	1.7 (14 V)	1.8 (10 V)
800 nm	11.2	7.2	11.4	8.0	23 (28 V)	24 (28 V)	1742	1711	7.7 (24 V)	7.3 (25 V)	1.3 (16 V)	1.6 (12 V)
1000 nm	17.7	10.4	17.7	11.2	18 (46 V)	44 (46 V)	1269	3676	7.1 (31 V)	8.4 (46 V)	0.8 (24 V)	1.2 (16 V)
1200 nm	20.0	11.6	19.8	12.7	33 (55 V)	165 (55 V)	2607	7986	7.7 (32 V)	9.6 (53 V)	0.8 (27 V)	1.0 (21 V)

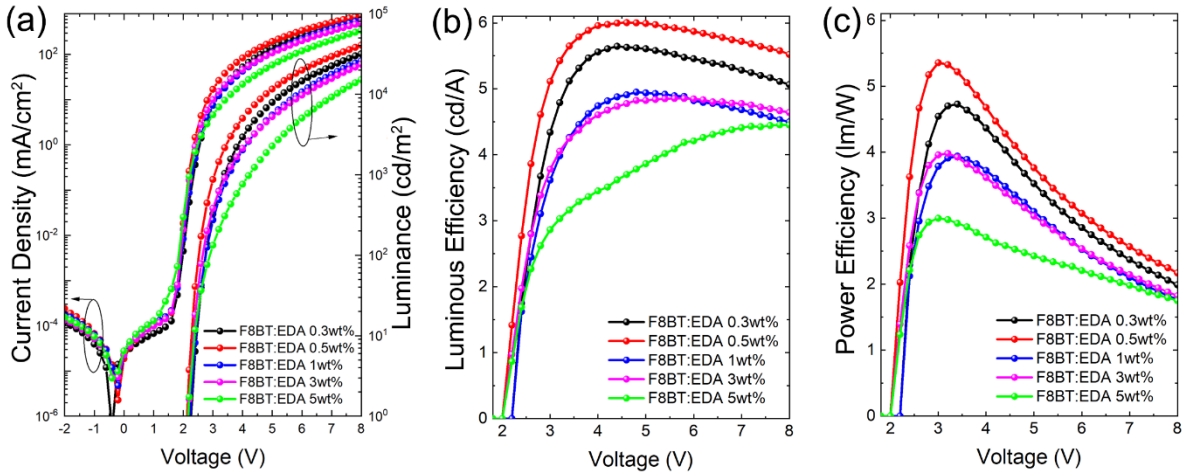


Figure S1. a) Current density-voltage-luminance (*J-V-L*) characteristics, **b**) luminous efficiency and **c**) power efficiency for 70-80-nm-thick F8BT:EDA PLEDs with various doping ratios from 0.3 wt% to 5 wt%. The F8BT with 0.5 wt% EDA PLED shows the highest luminance, luminous efficiency and power efficiency. Therefore, 0.5 wt% EDA was chosen for further PLED device studies to investigate the effect of F8BT thicknesses.

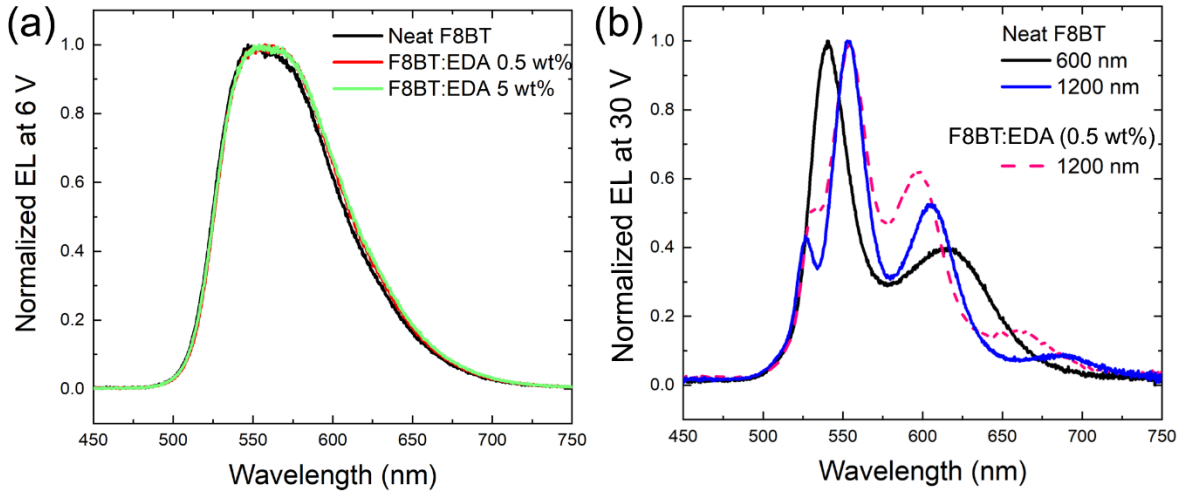


Figure S2. a) EL spectra of thin F8BT devices (70-80 nm) without and with EDA (0.5 and 5 wt%) at 6 V. **b**) EL spectra of thick F8BT devices without EDA (600 nm and 1200 nm) and with EDA (0.5 wt% EDA, 1200 nm) at 30 V. A significant microcavity effect that modifies that measured EL spectra is observed in thick devices. The EL appears to change with EDA doping in the thick device possibly indicating change in the recombination zone.

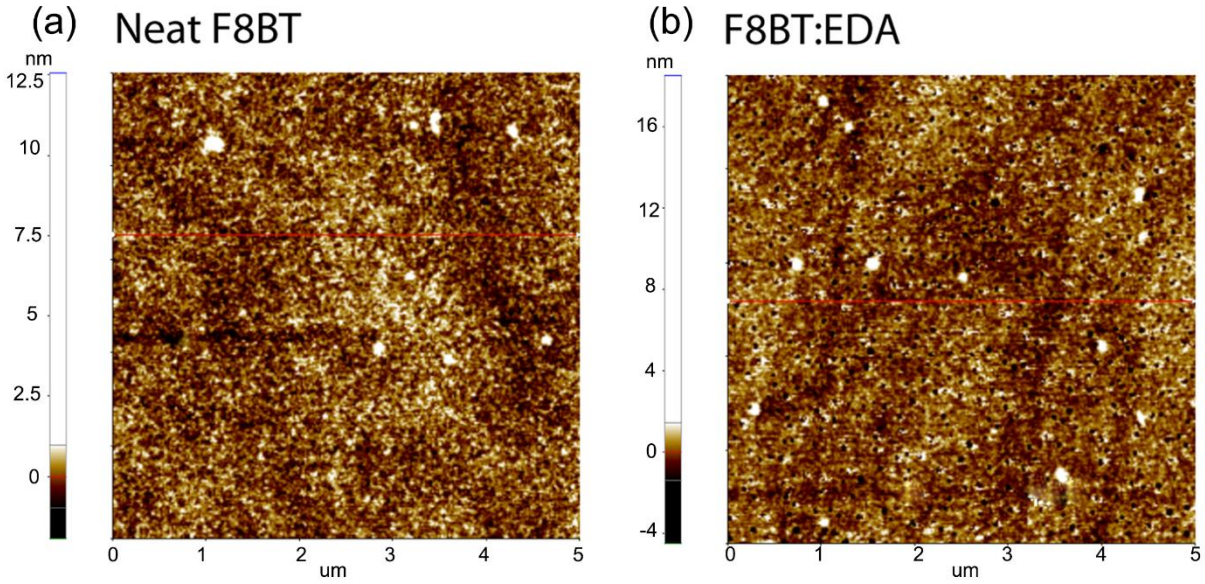


Figure S3. AFM images (5 µm × 5 µm) of (**a**) neat F8BT and (**b**) F8BT:EDA (0.5 wt%) (70 nm on quartz substrates). The films show similar and uniform morphologies. The surface roughness for neat F8BT and F8BT:EDA films is 0.49 nm and 0.72 nm, respectively.

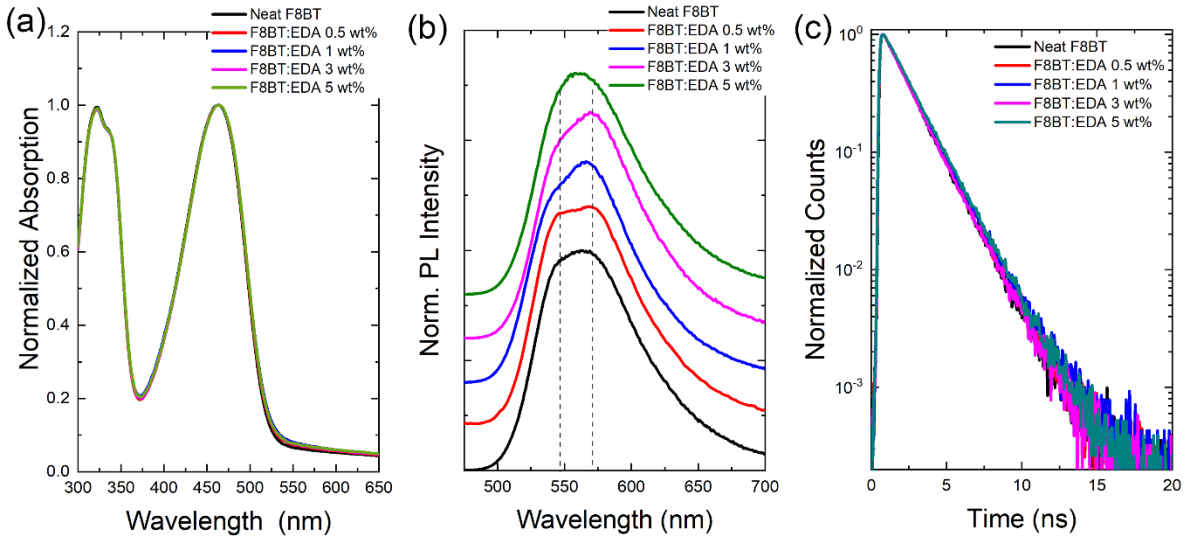


Figure S4. a) Normalized UV-Vis absorption spectra, **b**) normalized PL spectra with offset and **c**) transient characteristics (Ex: 404 nm, Em: 553 nm) of neat F8BT and F8BT:EDA thin films with different doping ratios ranging from 0.5 wt% to 5 wt% (70 nm thickness on quartz substrates). The EDA did not cause any noticeable changes in absorption spectra and transient PL characteristics, but small changes in relevant PL peak intensities at high EDA ratios were observed. The PLQYs for neat F8BT and F8BT:EDA (0.5 wt%) were 61 % and 69 % (±5 %).

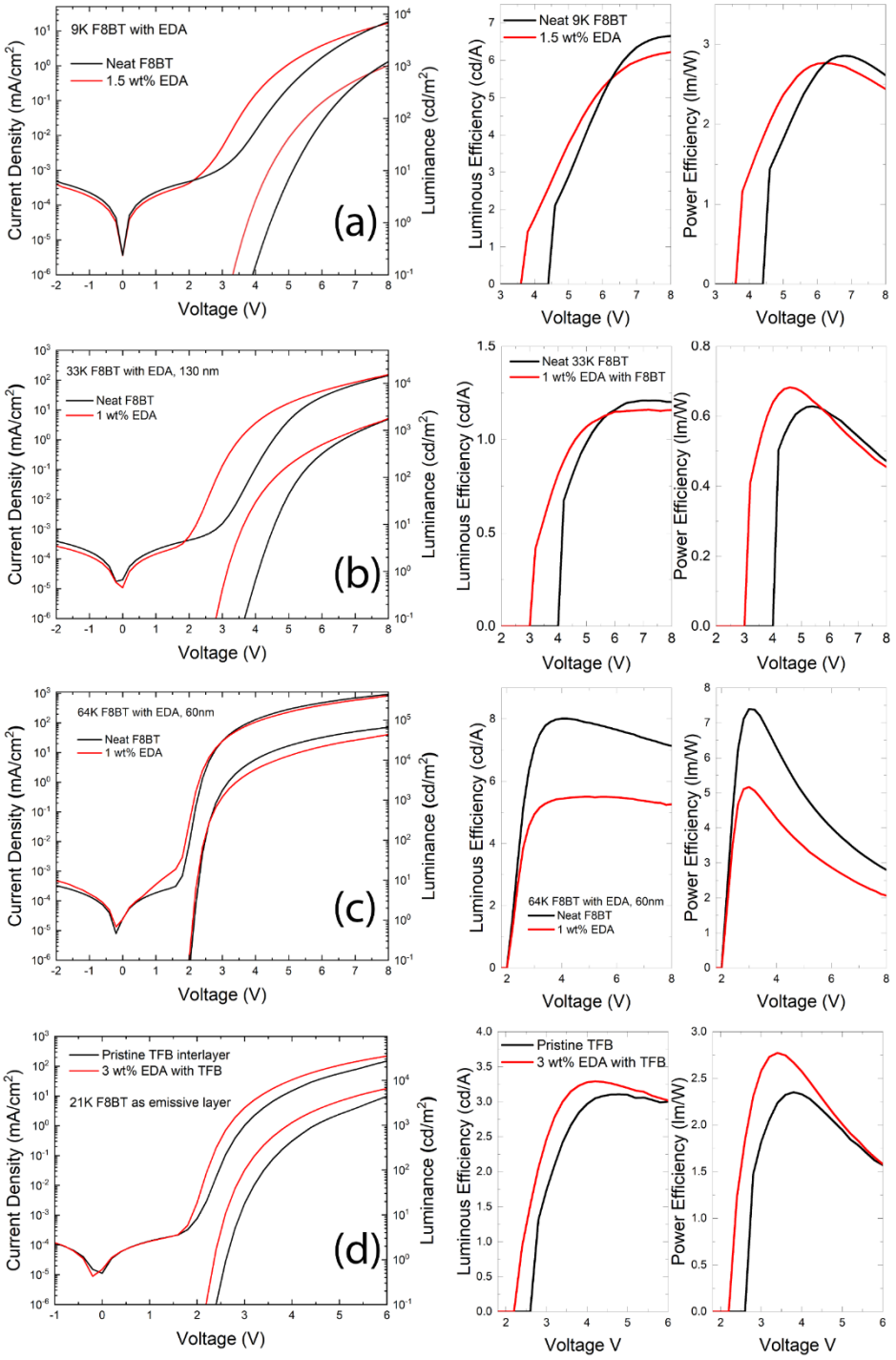


Figure S5. Molecular-weight dependent PLED performance for 9k (**a**), 33K (**b**) and 64K F8BT (**c**). Low MW F8BT, such as 9K-33K can work with EDA to reduce current and luminance turn-on voltages. **d**) JVL and efficiencies for 21K F8BT PLEDs with TFB interlayer with/without EDA. In this case, the EDA in TFB layer reduces turn-on voltages and improves device efficiencies.

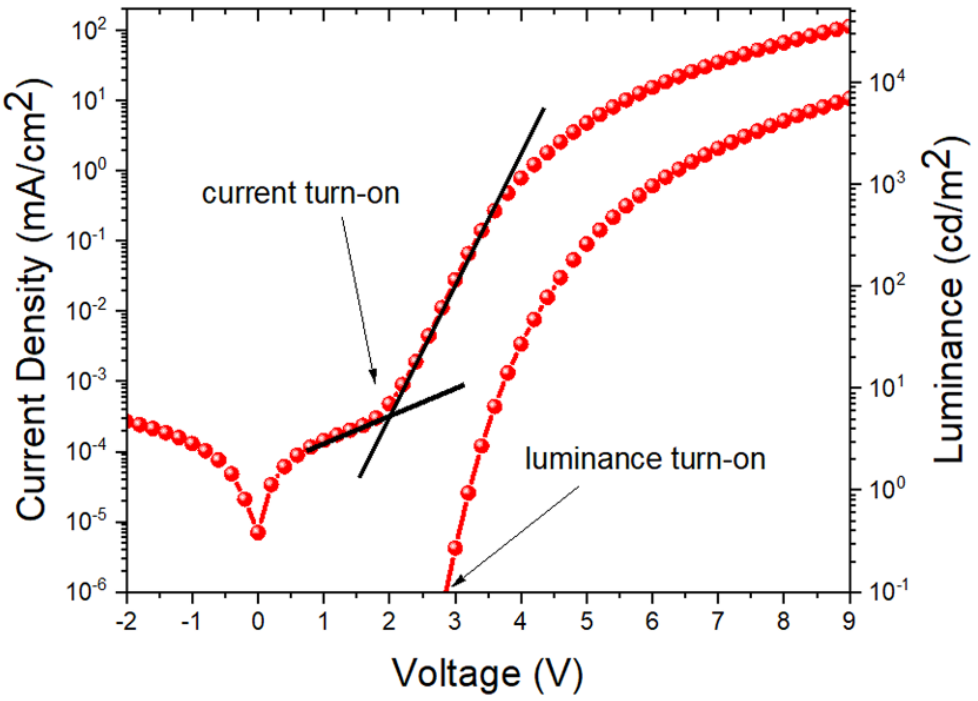


Figure S6. Typical *J-V-L* plot of a F8BT PLED. The turn-on voltage for current (V_J) is extracted from the crossing point in V when the slow and fast increases of the current coincide. The turn-on voltage for luminance (V_L) is extracted as the V required for 0.1 cd/m^2.

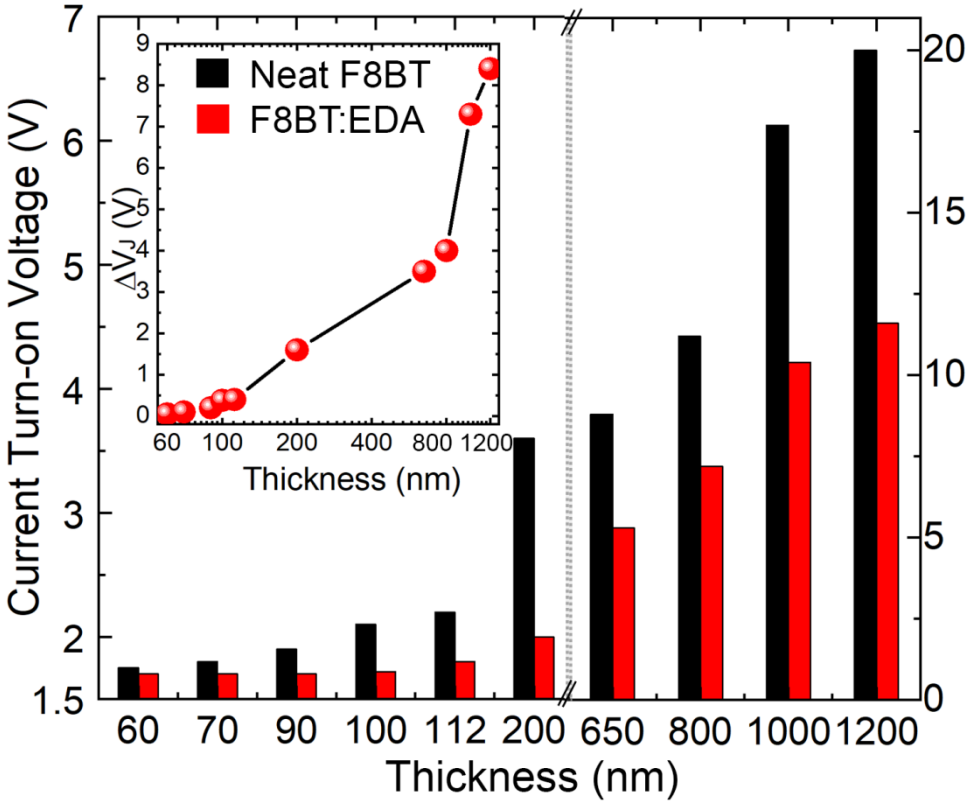


Figure S7. Turn-on voltages for current (V_J) as a function of thicknesses for neat F8BT and F8BT:EDA PLEDs. The inset graph shows the reduced turn-on voltages by EDA (ΔV_J) as a function of thicknesses. Note: The left Y-axis and right-Y-axis are for thin devices (60-200 nm) and thick devices (650-1200 nm), respectively.

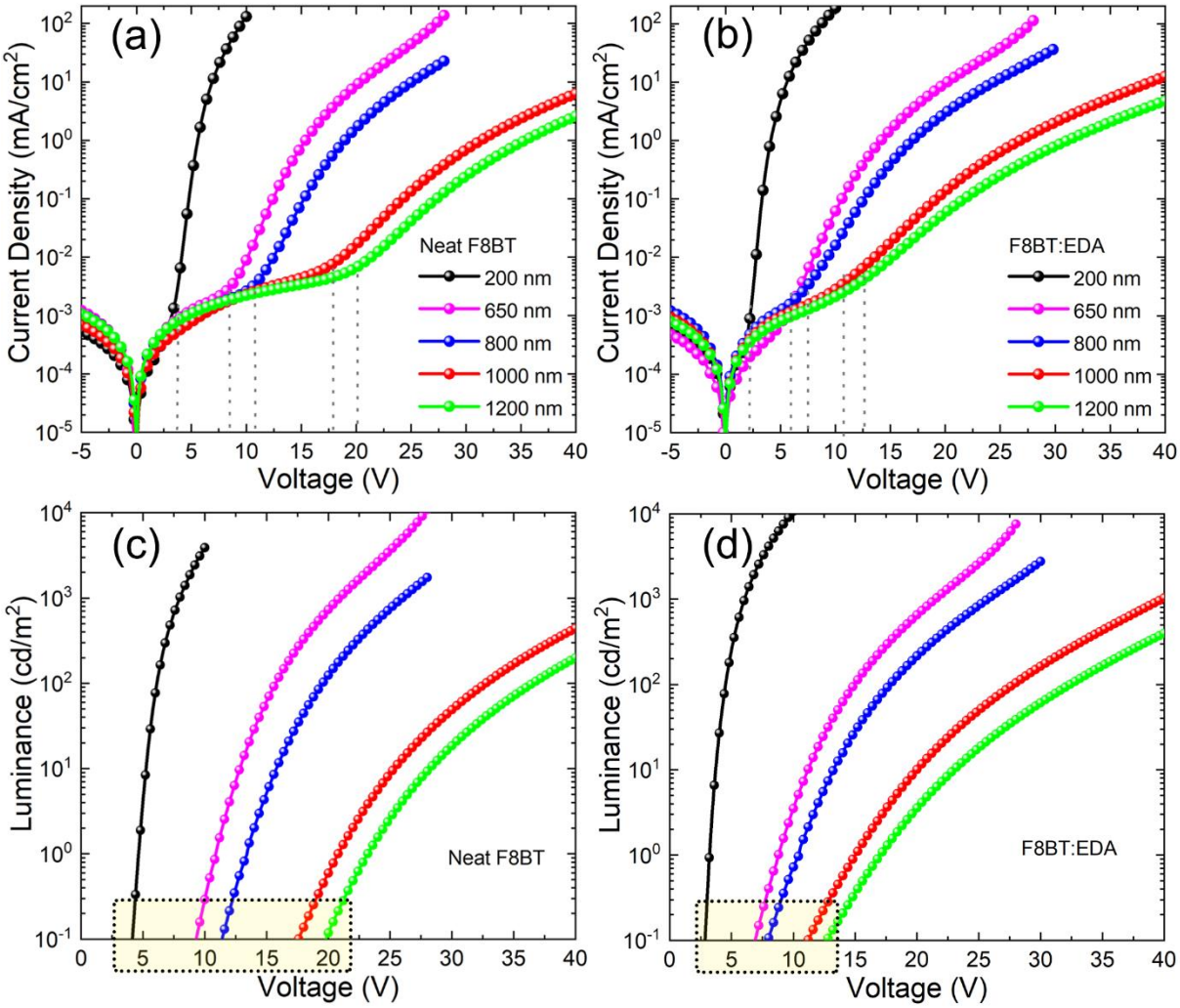


Figure S8. Current density-voltage and luminance-voltage characteristics for neat F8BT **(a, c)** and F8BT:EDA PLEDs **(b, d)** with thicknesses of 200 nm, 650 nm, 800 nm, 1000 nm and 1200 nm.

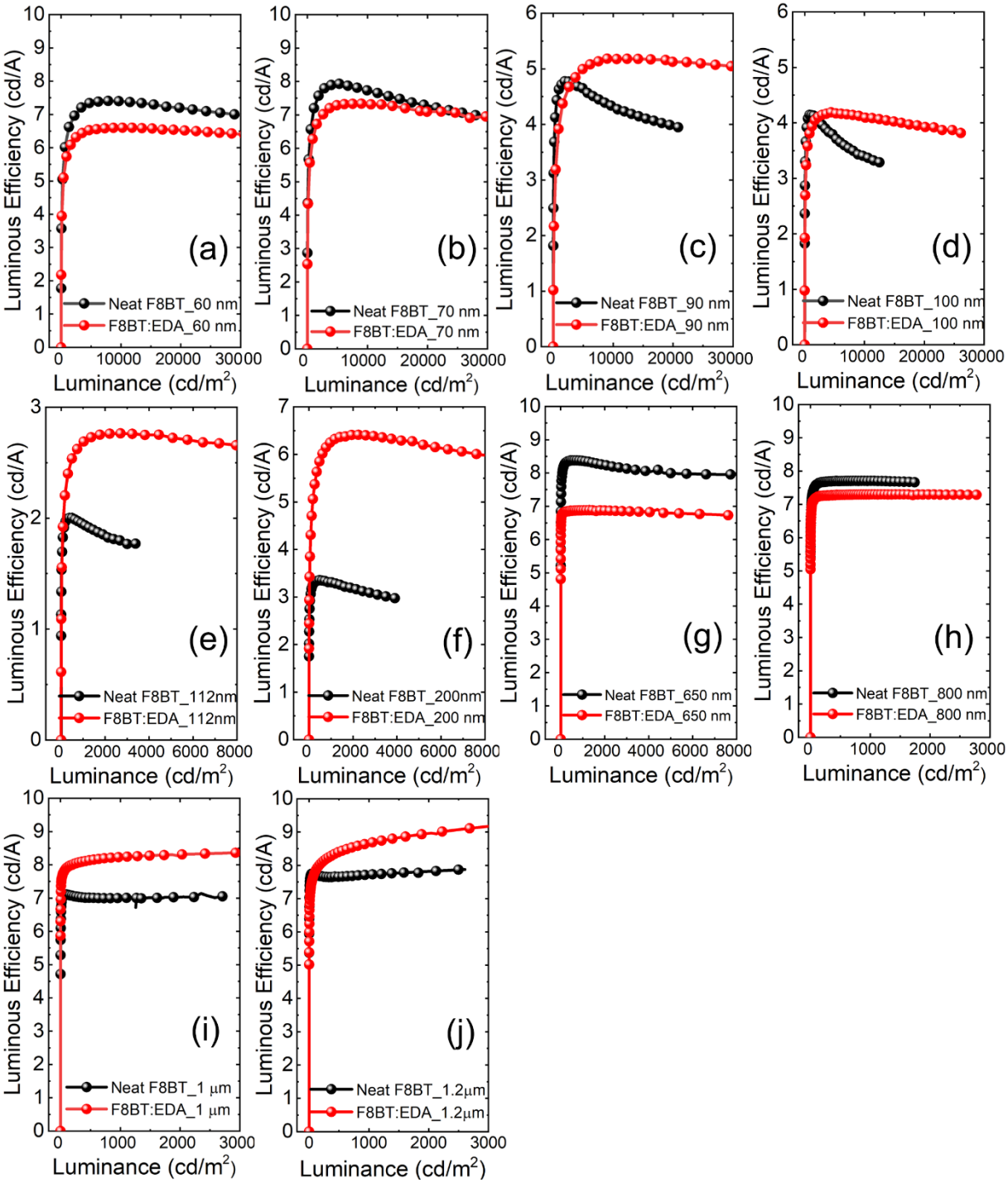


Figure S9. Luminous efficiency (cd/A) versus luminance (cd/m^2) for all devices tested (neat F8BT and F8BT:EDA PLEDs with different thicknesses ranging from 60 nm to 1.2 μm). Note that different scales are used for the x-axis (cd/m^2) and y-axis (cd/A).

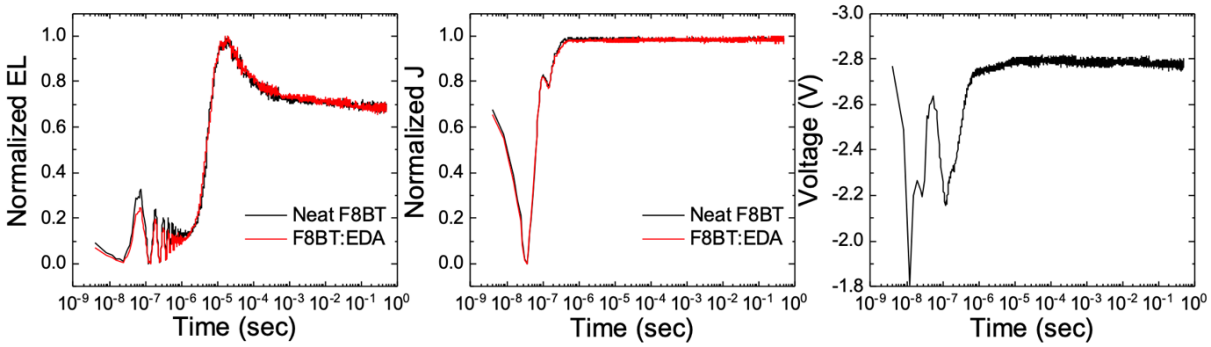


Figure S10. EL and current response time for neat F8BT and F8BT:EDA PLEDs under 2.8 V and 1 Hz. EDA dopant does not introduce any delays of EL and current injection.

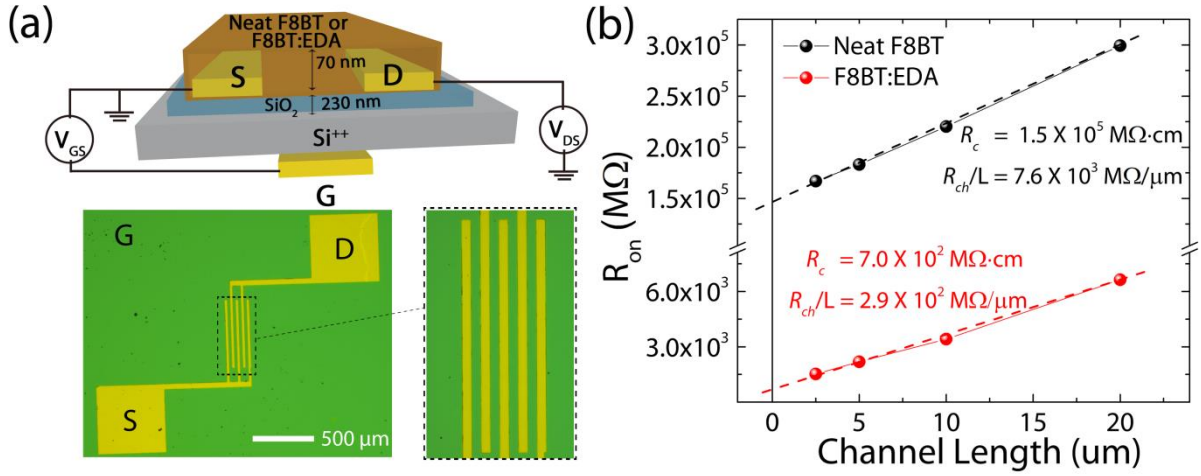


Figure S11. a) Schematic illustration of OFETs with F8BT and F8BT:EDA layers and photographs of the device taken by microscopy. **b**) The corresponding contact and channel resistance evaluated by the transfer line method (TLM) as a function of the channel length and gate and drain voltages, respectively. A significant improvement in the contact resistance is observed for the F8BT:EDA device.

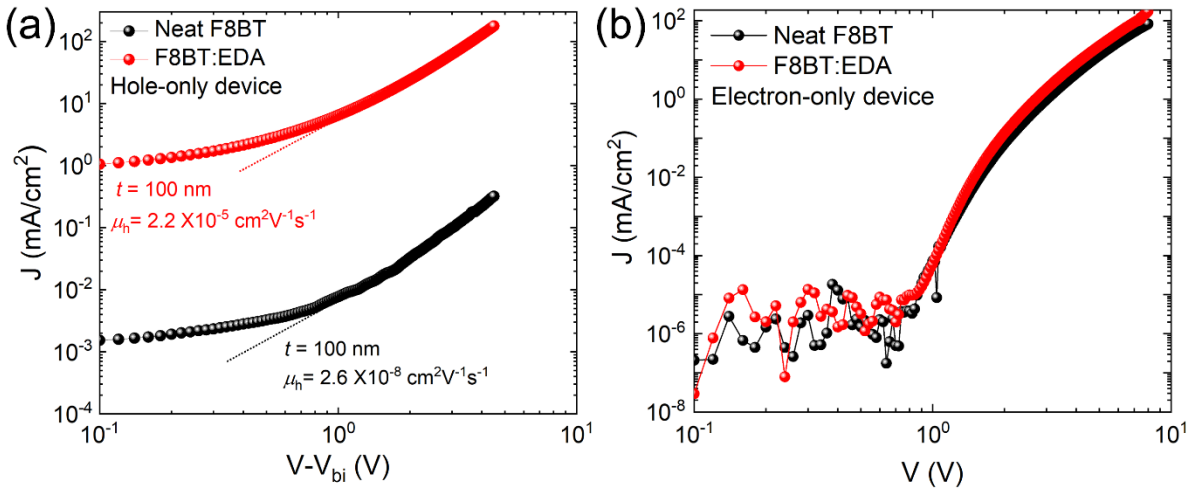
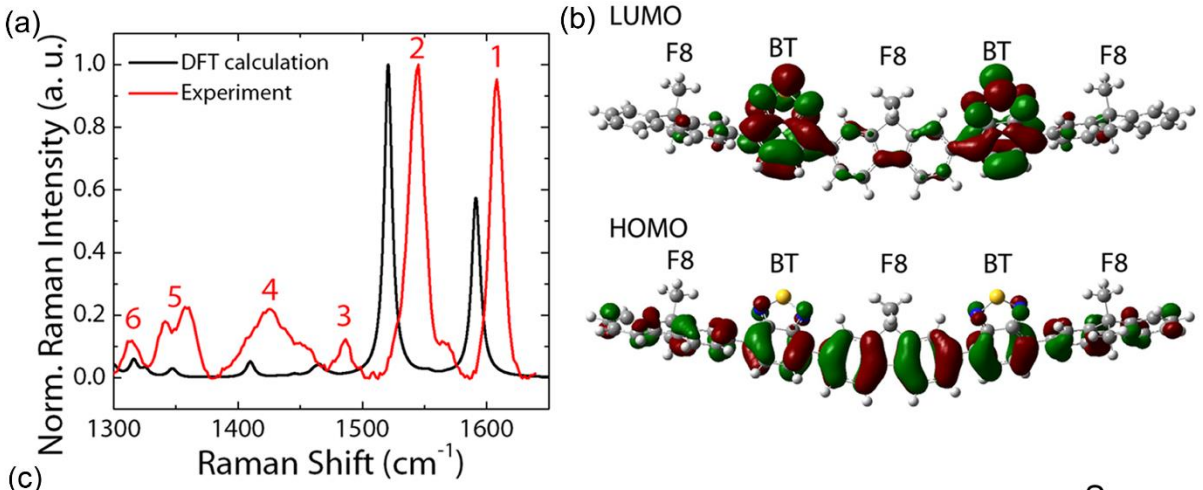


Figure S12. *J-V* characteristics of 100-nm-thick hole-only (ITO/PEDOT:PSS/TFB/ F8BT or F8BT:EDA /MoO_3/Au) (**a**) and electron-only (ITO/ZnO/ F8BT or F8BT:EDA /Ca/Al) devices (**b**), with 1.5 V built-in voltage (V_{bi}) for hole-only devices.



(c)

Peaks	Position (cm^{-1})	Vibrational mode assignments
1	1608	Ring stretching mode of F8 units (similar to 4, but symmetric)
2	1545	Ring stretching mode of BT units (symmetric)
3	1486	C-H wagging and C=C stretching mode of F8 units
4	1457 & 1425	Antisymmetric ring stretching mode of F8 units
5	1357	C-C bond stretching of BT units
6	1314	C-C bond stretching and ring breathing of F8 units

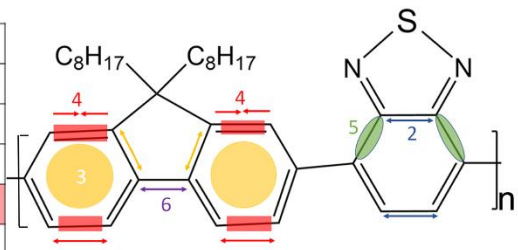


Figure S13. a) Measured and simulated Raman spectra of F8BT. For simulation, DFT with a 6.31G(d. p) basis set was used on F8BT oligomer with methyl side groups. **b**) Simulated HOMO and LUMO wavefunctions of F8BT. **c**) Assignments of the main Raman peaks of F8BT.

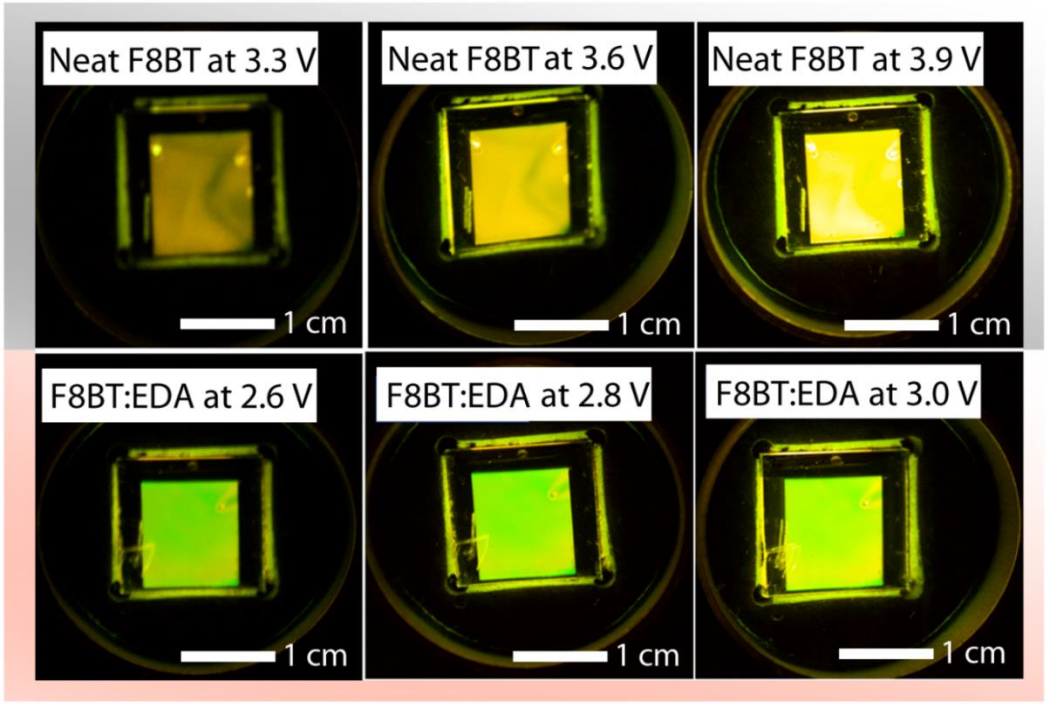


Figure S14. The neat F8BT device shows nonuniform and voltage-dependent emission, whereas the F8BT:EDA device shows an electroluminescence uniformity for large-area PLED devices (1 cm × 1 cm, 112-nm thickness) under different applied voltages.

We investigated the homogeneity and uniformity of the light-emitting properties of the corresponding PLEDs, which are critical parameters for facilitating printing technologies (i.e., inkjet printing and slot-die machines) of large-area and high-performance PLEDs.[1] We prepared high-concentration F8BT and F8BT:EDA solutions (21 mg/ml) to fabricate large-area (1 cm × 1 cm) devices with a 112-nm-thick emitting layer, as shown in **Figure S14**. The neat F8BT PLEDs did not show uniform light emission throughout the entire device above the turn-on voltage (V_L = 3.3 V at 1 cd/m^2) due to inhomogeneities in the film thickness. These features were consistent with the thickness-dependent light-emitting properties observed in neat F8BT PLEDs (60-112 nm, **Figure 2**). The F8BT:EDA PLEDs showed very homogeneous and uniform light emission over the entire area (V_L = 2.4 V at 1 cd/m^2). The homogeneous light emission in the F8BT:EDA PLEDs at the V_L could arise from their thickness-independent turn-on voltage and the minimization of the efficiency roll-off. The emission color difference might

indicate a shift in the recombination zone or a weak microcavity effect induced by the addition of the EDA to the F8BT emissive layer.[2]

References

[1] Singh, M., Haverinen, H. M., Dhagat, P. & Jabbour, G. E. Inkjet printing-process and its applications. *Adv. Mater.* **2010**, *22*, 673-685.

[2] Bulovic, V., Khalfin, VB., Gu, G., Burrows, PE., Garbuzov, DZ., Forrest, SR. Weak microcavity effects in organic light-emitting devices. *Phys. Rev. B.* **1998**, *58*, 3730-3740.